Measurements of Three-Dimensional Turbulent Flow Behind a Propeller in a Shear Flow

M.A. Kotb* and J.A. Schetz†
Virginia Polytechnic Institute and State University, Blacksburg, Virginia

This paper presents detailed measurements close behind a 0.49 m (1.615 ft), three-bladed propeller tested in the Virginia Polytechnic Institute and State University 2×2 m (6×6 ft) wind tunnel. Tests were run with a uniform approach flow as a baseline, and then the main test series was run with a variable mesh wire grid upstream to produce an approach flow with an essentially linear velocity gradient. The results are compared to elucidate the effects of the nonuniform approach flow. Several types of measurements are reported. First are gross quantities such as overall thrust and torque. The second type of measurements are mean (in the turbulence sense) quantities obtained with a five-port yawhead tube. All three components of the mean velocity and static pressure were obtained. The third type of measurements were made with an x-wire anemometer and an rms meter. These measurements yield all components of the turbulence intensities and stresses at a point averaged over many passes of the propeller blades. The last type of measurements were performed with the x-wire and a microcomputer. The computer is triggered to record many (approximately 160) traces from individual blade-passing events. These measurements are then processed to yield profiles of the mean velocities and turbulence intensities and stresses behind an individual blade.

Nomenclature

C_{p_S} = static pressure coefficient, $=(P_s-P_\infty)/q_\infty$
D = propeller diameter
J = advance coefficient, $=U_\infty/ND$
K_T = thrust coefficient, $=T/(\rho_\infty N^2D^4)$
K_Q = torque coefficient, $=Q/(\rho_\infty N^2D^5)$
N = rotational speed, rev/s
P_s = local static pressure
P_∞ = freestream static pressure
P/D = propeller pitch-diameter ratio
q_∞ = freestream dynamic pressure, $=\frac{1}{2}\rho_\infty U_\infty^2$
Q = torque
R = propeller radius
Re_c = Reynolds number at 0.7 propeller radius, $=V_Rc_{0.7}/\nu$
T = thrust
U = mean axial velocity
U_{CL} = upstream velocity at the centerline
U_∞ = freestream velocity
u' = fluctuating component of axial velocity
$\overline{u'v'}, \overline{u'w'}, \overline{v'w'}$ = velocity correlations in the Cartesian coordinate system
$\overline{u_1'v_1'}, \overline{u_1'w_1'}, \overline{v_1'w_1'}$ = velocity correlations in the cylindrical coordinate system
$\sqrt{\overline{u'^2}}/U$ = axial turbulence intensity
V = mean velocity component in the Y direction
V_R = resultant velocity at 0.7 propeller blade radius, $=U_\infty\sqrt{1+(0.7\pi/J)^2}$
v' = fluctuating component of the Y velocity component
v_1' = fluctuating component of the radial velocity component
$\sqrt{\overline{v'^2}}/U$ = turbulence intensity in the Y direction
$\sqrt{\overline{v_1'^2}}/U$ = turbulence intensity in the radial direction
W = mean velocity component in the Z direction
w' = fluctuating component of the Z velocity component
w_1' = fluctuating component of the tangential velocity component
$\sqrt{\overline{w'^2}}/U$ = turbulence intensity in the Z direction
$\sqrt{\overline{w_1'^2}}/U$ = turbulence intensity in the θ direction
X, r, θ = axial, radial, and tangential coordinate directions
X, Y, Z = axial, transverse, and vertical coordinate directions
ν = kinematic viscosity
ρ_∞ = freestream density

Introduction

THE aero/hydrodynamics of propellers has been the subject of study for many years. Much of the work has been concerned with blade design, often in a uniform approach flow, and the analyses are usually inviscid. The effects of nonuniform inflow are commonly treated by a single gross parameter such as the "wake fraction," at least for ship propellers.

Recently, for several reasons, there has been considerable interest focused on the viscous flow in the immediate vicinity of the propeller. First, it is recognized that propeller/body (hull or fuselage) interactions are important for propeller design, noise generation, and vibrations. Second, the wake behind a propeller is of interest for noise, control surface effectiveness, and possible vehicle detection. In order to analyze the wake, it is necessary to have accurate "initial conditions" just behind the propeller disk.

This work addresses the flowfield near a propeller operating in a nonuniform approach flow experimentally. The particular type of nonuniformity selected is a linear velocity gradient (e.g., a "shear" flow). This choice was

Presented as Paper 84-1676 at the AIAA 17th Fluid Dynamics, Plasmadynamics and Lasers Conference, Snowmass, CO, June 25-27, 1984; received Aug. 8, 1984; revision received June 14, 1985.

*Graduate Assistant, Department of Aerospace and Ocean Engineering.
†Professor and Department Head, Department of Aerospace and Ocean Engineering. Fellow AIAA.

made because it represents a first systematic step beyond a uniform flow.

Another feature of interest is the flow in the wake behind individual blades. That information is useful in blade design and in assessing overall performance. The present study also considers that aspect of the flow.

Four techniques, varying in level of sophistication and accuracy and amount of information each can yield, were applied throughout this study. The first technique was the direct measurement of forces and moments. To more fully understand these data it was necessary to measure the propeller-induced flowfield. A five-hole yawhead probe and a hot wire were used for mean flow and turbulence information for the second and third methods. The results obtained through this step have the limitation of being mean in both time and space. In particular, they are averaged over the propeller disk at a given radial location—they include many blade-passing events. With the introduction of microprocessors it is now possible to measure the spatial distribution of all flowfield quantities, which was the aim of the fourth class of techniques used.

The four methods were first applied for a propeller in uniform flow. Then, linearly sheared flow was chosen to represent a nonuniform incident flow.

The testing was conducted in a wind tunnel at a free stream velocity of 8.52 m/s (27.95 ft/s) resulting in a Reynolds number, Re_c of 0.55×10^5. This velocity value was selected based on the drive motor, propeller blade strength, and tunnel limitations. This Re_c value also was used in previous studies.[1-5] A detailed discussion about the effect of blade Reynolds number on separation was given by the present authors in Ref. 6. The main point made was that calculations and studies of previous data indicate that the flow over these blades at these conditions is not separated. The blade tip Mach number was maintained below 0.1 to stay away from compressibility effects.

Apparatus and Instrumentation

Facilities

The Virginia Polytechnic Institute and State University (VPI & SU) 2×2 m (6×6 ft) wind tunnel was used. The tunnel has a very low level of background turbulence; less than 0.3% for the uniform flow case and 0.7% in the shear flow case. The linear shear flow is generated by placing a combination of five wire screens of different cross tunnel wire distribution upstream of the test section. See Fig. 1.

A survey of the flow upstream of the propeller was made to give the distribution of velocity and turbulence intensity. The velocity gradient (slope) was found to be 0.0794. The screens used to shear the flow were found to have a small and acceptable effect on the upstream turbulence level.[11]

Model

The three-bladed propeller was constructed from a cut-up, 0.508-m (1.667-ft) diameter maple model airplane propeller (Zinger 20-6). The wooden hub was removed and replaced by an aluminum one. Each blade was clamped to the hub with a steel disk that could be rotated in 18-deg intervals. A streamlined aluminum spinner cap was mounted on the shaft.

Blade thickness, maximum camber, chord length, and blade angles were carefully measured at 10 radial stations (See Table 1.) The test apparatus provides a means of measuring propeller thrust and rpm. Assembly details are given in Ref. 11.

Instrumentation

A straight, three-dimensional yawhead (five-hole) probe, manufactured by the United Sensor Corporation, was used to obtain mean flow measurements.

Turbulent flow measurements were obtained using an x-wire array probe with a two-channel constant-temperature anemometer (TSI Model 1050) and a two linearizers (TSI Model 1052). The signal was recorded by an integrater and an rms voltmeter.

For the flowfield measurements behind individual blades, a microcomputer was used to acquire and save instantaneous data over a number of blade-passing events. The data was sampled at a rate of 28K (samples per second). Software was written to replace the dc and rms meters.

Data Reduction

The data taken by the yaw probe was reduced using calibration following Lee.[7] Hot-wire response equations derived by Champagne and Sleicher[8] were used. At a particular point, the x-wire readings were taken in three different wire orientations, i.e., horizontal, vertical, and diagonal (45 deg). A computer program was written to use these data as input. The program output represents the three components of the mean velocity vector and the six different components of the Reynolds stress tensor at this point.

For the individual blade wake studies, a stationary x wire together with an averaging technique were used. A complete error analysis associated with the various types of measurements and instruments used throughout this study is given in Ref. 11.

Results

Propeller Performance

The three-bladed propeller with $P/D = 1.572$ was tested with uniform and shear upstream flows. Performance results

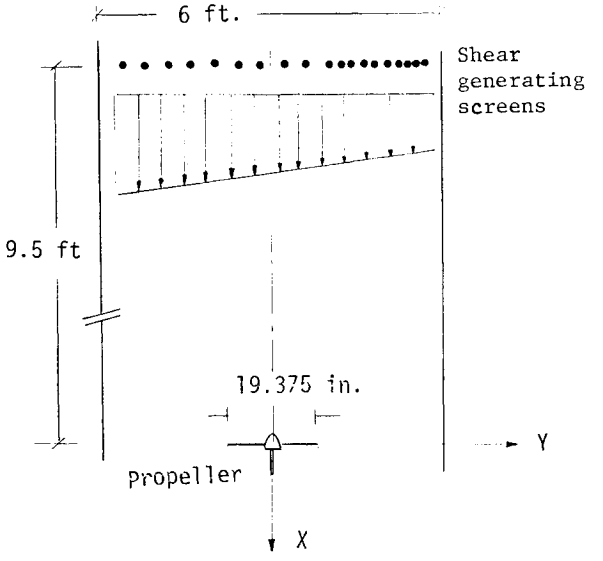

Fig. 1 Wind tunnel test configuration.

Table 1 Propeller geometry

Radius, cm	Chord, cm	Blade angle, deg	Maximum thickness, cm	Maximum camber, cm
3.69	2.911	54.0	0.95	0.392
4.92	3.286	51.013	0.913	0.368
7.92	3.875	46.139	0.853	0.323
9.84	4.253	41.939	0.786	0.279
12.30	4.419	38.413	0.711	0.237
14.76	4.374	35.562	0.628	0.196
17.22	4.117	33.386	0.537	0.158
19.69	3.649	31.883	0.438	0.121
22.15	2.969	31.055	0.332	0.086
24.60	2.078	30.902	0.218	0.053

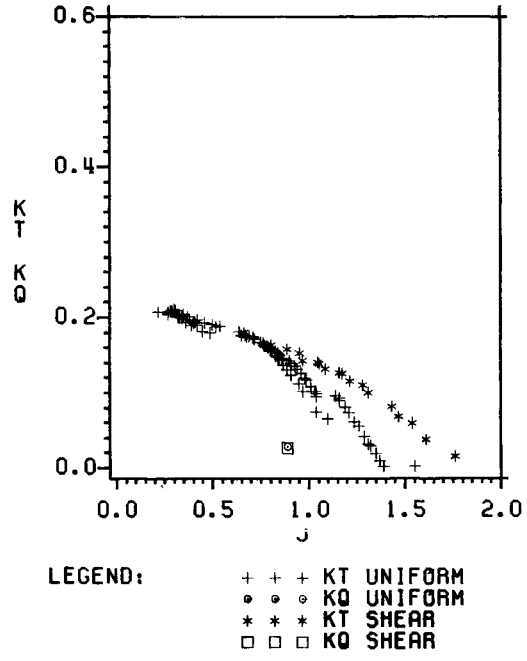

Fig. 2 Three-bladed, 1.572 P/D ratio propeller performance in uniform and shear flows.

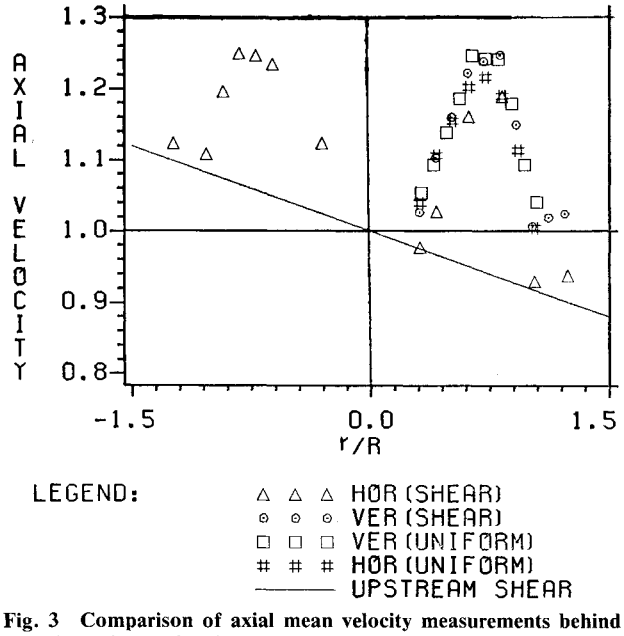

Fig. 3 Comparison of axial mean velocity measurements behind a three-bladed, 1.572 P/D propeller in uniform and shear approach flow cases at $X=0.025D$.

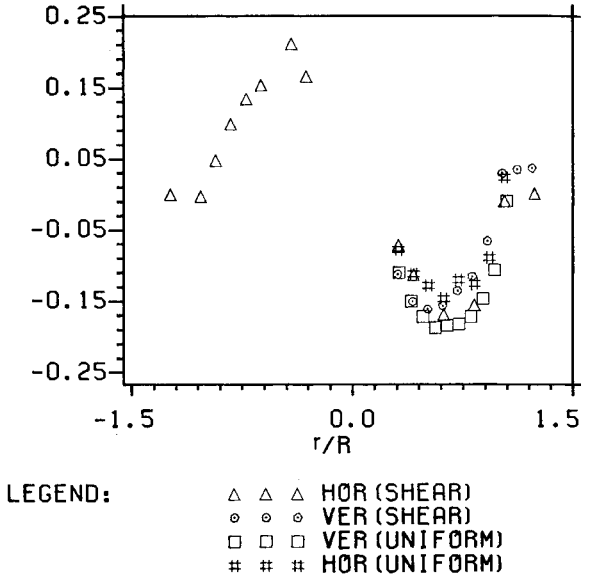

Fig. 4 Comparison of swirl mean velocity measurements behind a three-bladed, 1.572 P/D ratio propeller in uniform and shear approach flow cases at $X=0.025D$ and $J=0.899$.

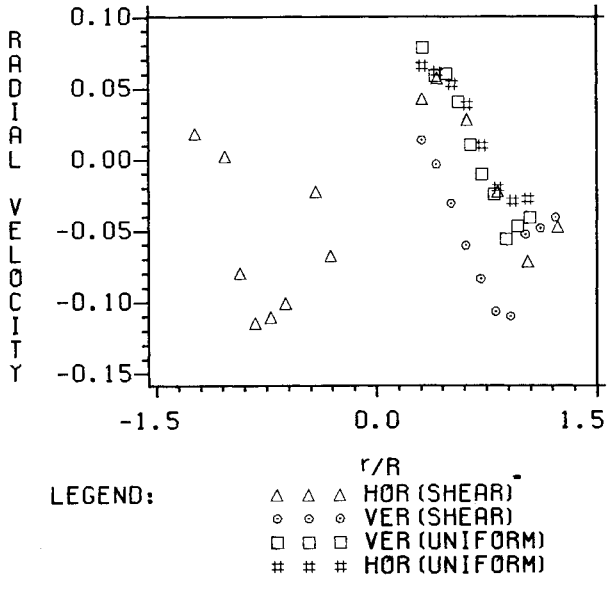

Fig. 5 Comparison of radial mean velocity measurements behind a three-bladed, 1.572 P/D ratio propeller in uniform and shear flow cases at $X=0.025D$ and $J=0.899$.

are given in the usual dimensionless form in Fig. 2. For the shear flow test case, the centerline velocity (8.52 m/s) was used to calculate the corresponding advance coefficient. A look at the performance results under uniform and shear flow conditions reveals that a slightly higher effective pitch ratio was observed in the shear flow case. The results for the two cases diverge for the thrust coefficient after $J=0.9$. At the selected test J value of 0.899 (1150 rpm), the thrust coefficient was 0.135 in uniform flow and 0.158 for shear flow. The torque coefficients were 0.0279 and 0.0269 for the uniform and shear flow cases, respectively.

Mean Velocities and Pressures

It is interesting to first observe the variation of the mean axial velocity at $X/D=0.025$ along the horizontal axis for two reasons (see Fig. 3): 1) the upstream flow is horizontally sheared, and 2) a direct comparison with the uniform flow case can be made. The maximum normalized induced axial velocity in the shear flow case is about 0.24 located at $0.8R$, whereas it is 0.22 for the uniform case at $0.7R$. Results of the distribution along the vertical plane also are shown on the same plot for the two cases. Once again, the sheared flow case experienced higher induced velocity (0.30) than the uniform case (0.25).

The plot in Fig. 4 shows that the swirl velocity is slightly higher on the higher upstream velocity side ($Y/R<0$) than on the other side ($Y/R>0$) along the horizontal axis. The swirl imparted to the flow, for all cases, varies between 15 and 20% of the freestream velocity. In the shear flow case, the swirl is lower in the vertical plane than in the horizontal.

The vertical distribution of radial induced velocity in the shear case shows more flow contraction due to propeller ac-

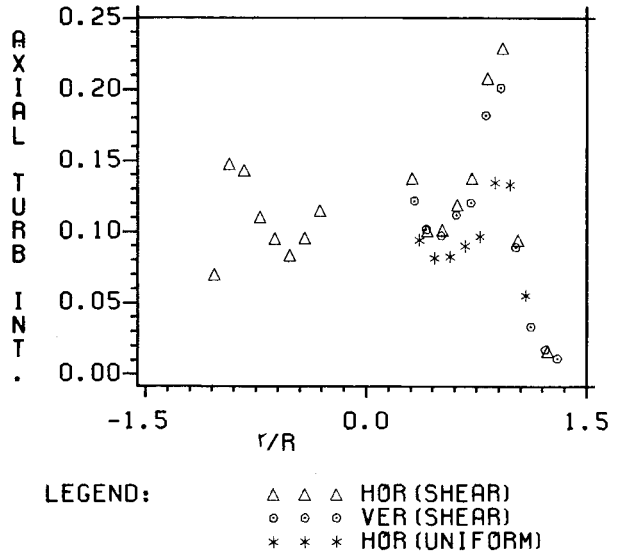

Fig. 6 Comparison of axial "turbulence" intensity measurements behind a three-bladed, 1.572 P/D ratio propeller in uniform and shear flow cases at $X=0.025D$ and $J=0.899$.

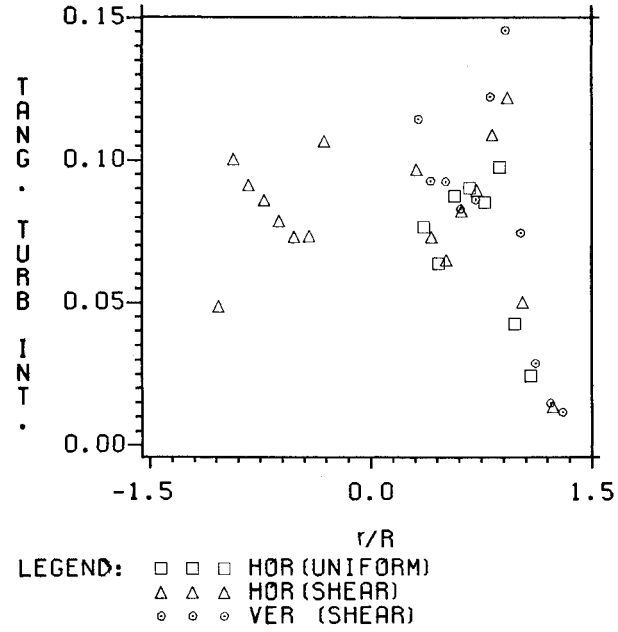

Fig. 7 Comparison of tangential "turbulence" intensity measurements behind a three-bladed, 1.572 P/D ratio propeller in uniform and shear flow cases at $X=0.025D$ and $J=0.899$.

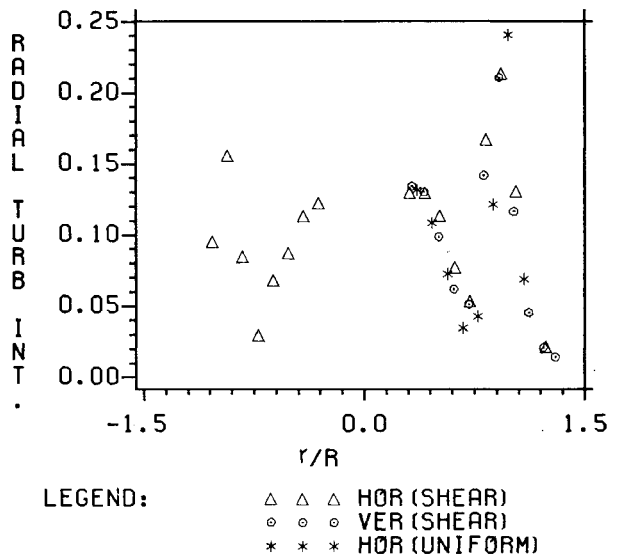

Fig. 8 Comparison of radial "turbulence" intensity behind a three-bladed, 1.572 P/D ratio propeller in uniform and shear flow cases at $X=0.025D$ and $J=0.899$.

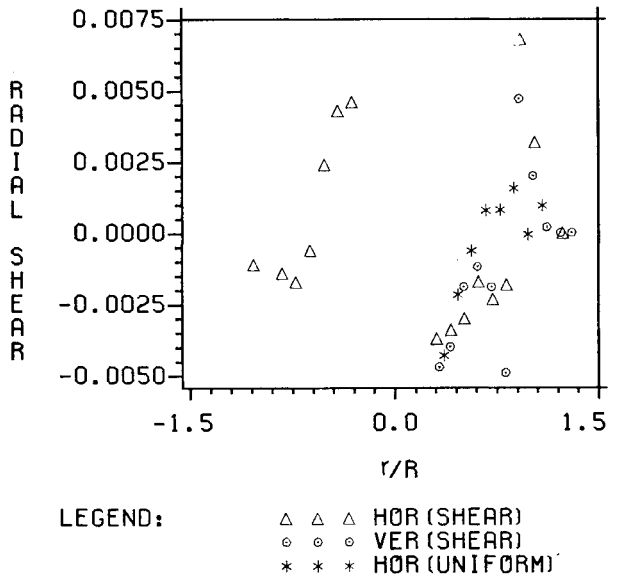

Fig. 9 Comparison of "Reynolds stress" ($\overline{u_1'v_1'}$ component) behind a three-bladed, 1.572 P/D ratio propeller in uniform and shear flow cases at $X=0.025D$ and $J=0.899$.

tion, as can be seen in Fig. 5. The maximum value reaches about 11% of the freestream velocity, whereas it is only 6.5% for the horizontal distribution.

Turbulence

"Turbulence" quantities measured by a hot wire and an rms meter, as reported in Figs. 6-11, are composed of several components: a periodic component at the blade-passing frequency, a component generated in the boundary layer over the blades, a component generated across the shed vortex sheet, and finally turbulence imbedded on the onset flows. The measured quantities that include all of these components will be termed herein global "turbulence" in order to distinguish them from simple turbulence in shear flows.

In order to decompose the periodic component, an ensemble-averaged method was used to reduce the conditionally sampled raw data for the blade wake measurements. The periodic components of the blade rate were removed. Hence, the turbulence in the usual sense, which was superimposed on the mean value, was obtained as given in Figs. 12-17. The detailed data reduction procedure is given in Ref. 11.

The axial global "turbulence" intensity distribution along the horizontal axis is shown in Fig. 6. These data are normalized with the local axial velocity. The shear flow profiles are characterized by two peaks at $\pm R$. The right peak (at $Y/R=+1.0$) is higher (25%) than the one at the left ($Y/R=-1.0$), which is 15%. The distribution along the vertical axis is plotted on the same graph. The values are almost identical with the horizontal distribution except for a lower peak value (21%). The uniform flow data show only a 15% maximum value at $0.95R$.

Tangential "turbulence" intensity distributions in Fig. 7 show more or less symmetric horizontal profiles with peaks at $\pm R$. Vertical distributions show a similar profile except

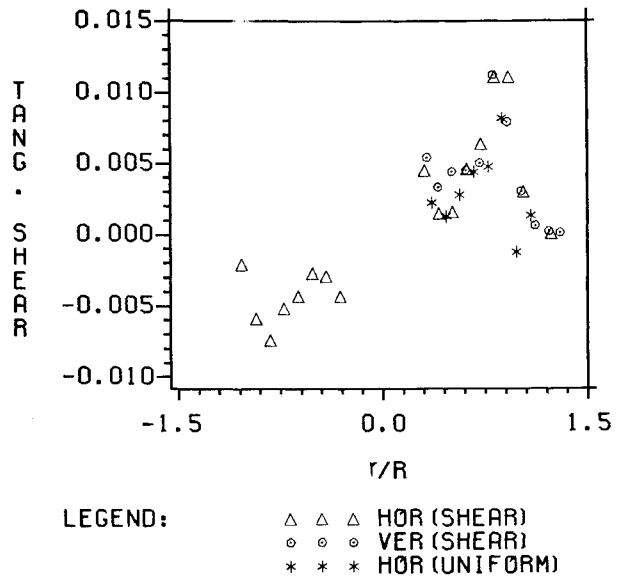

Fig. 10 Comparison of "Reynolds stress" ($\overline{u_1'w_1'}$ component) behind a three-bladed, 1.572 P/D ratio propeller in uniform and shear flow cases at $X=0.025D$ and $J=0.899$.

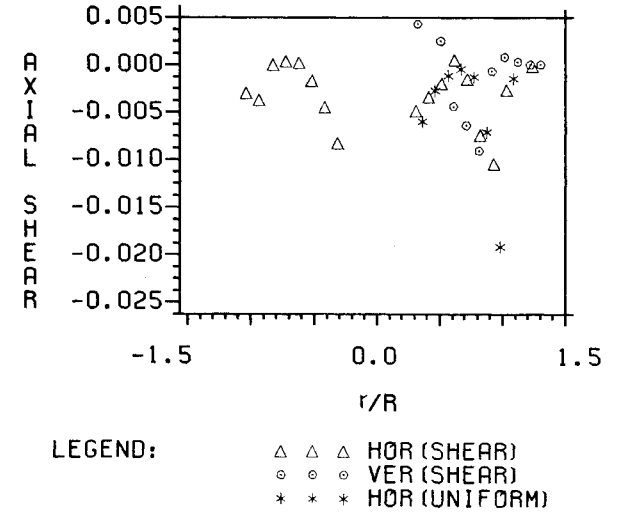

Fig. 11 Comparison of "Reynolds stress" ($\overline{v_1'w_1'}$ component) behind a three-bladed, 1.572 P/D ratio propeller in uniform and shear flow cases at $X=0.025D$ and $J=0.899$.

for an 18% higher peak. The uniform flow data shows lower values than either horizontal or vertical cuts in the shear flow.

The radial "turbulence" profiles given in Fig. 8 show two peaks at $\pm 0.95R$. The peak at the right side ($Y/R>1.0$) appears higher due to the way they have been normalized. However, if centerline velocity is used for normalization, the plots will be the same (about 18%). Sheared flow data compares very well in shape with the uniform case except that the latter has 14% higher peak values. Vertical and horizontal distributions assume the same functional shape as well as magnitude. The tangential turbulence intensity has the lowest level among the three components.

Horizontal and vertical profiles of the global radial Reynolds stress component $\rho u_1' v_1'/\rho_\infty U^2$ are shown on Fig. 9. The two profiles have peaks around the tip. The horizontal peak is 7×10^{-3}, whereas the vertical peak is 5×10^{-3}. The uniform inflow results are quite low—the maximum value was 1.5×10^{-3}. For the three profiles, this shear-stress component changes sign when moving toward the hub; the minimum value is about -4.5×10^{-3}.

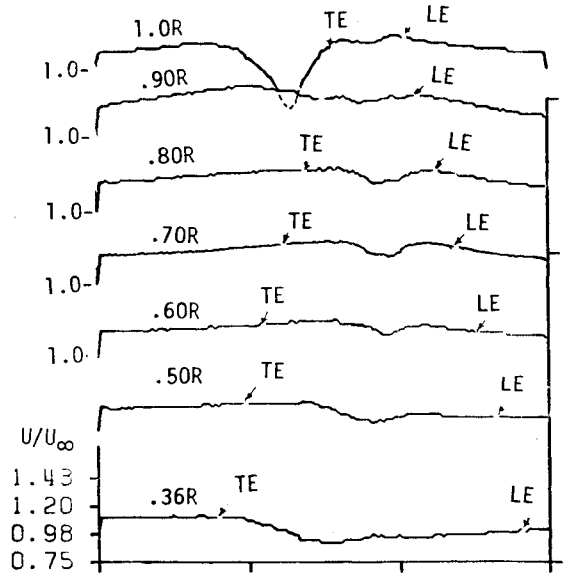

Fig. 12 Axial mean velocity profiles behind a propeller blade in uniform flow at $J=0.899$.

The global tangential stress component, $\rho\overline{u_1'w_1'}/\rho_\infty U^2$, distributions are given in Fig. 10. The vertical profile is slightly different from the horizontal profile, however, both have the same maximum level value (0.0105) at the same radial location, $0.9R$. Results from the uniform flow case were plotted on the same graph. The profile is narrower, and the peak value is less at 8.5×10^{-3} at $0.9R$.

The third global Reynolds stress component, $\rho\overline{v_1'w_1'}/\rho_\infty U^2$, profiles are shown on Fig. 11. Both the horizontal and vertical distributions look the same except that the latter is shifted toward the hub. The uniform entry flow case is also functionally the same, however, the peak values are almost twice as high at the tip.

Individual Blade Flowfields

In order to yield statistically accurate time-averaged quantities, the raw data should be acquired and saved over an ample period of time. With the method used herein, that translates into a sufficient number of sweeps across the blade wake. In the present study a "sufficient" number was selected with two factors in mind: 1) the large storage space required for this much data, and 2) the errors involved in finite sampling procedures. Three flow quantities were chosen for examining these kinds of errors. Those chosen were the axial velocity ratio U/U_∞, the axial turbulence intensity $\sqrt{\overline{u'^2}}/U$, and the velocity correlation function $\overline{u'v'}/U^2$, all at a radial position of $0.6R$.

The data were averaged for a systematically varying number of sweeps. For the mean velocity, the results show almost no change over the range from 120 to 160 sweeps. References 9 and 10 permit estimating the error for such calculations to be less than 1.6% in the mean velocities for a turbulence level of 20% and 160 sweeps. For this number of sweeps, the same references give an 11% error estimate for turbulence quantities. Our calculations show constancy in the profiles over the 120-150-sweep range. The Reynolds stress results show that the calculations are quite sensitive to the number of sweeps, particularly in the 20-100-sweep range. However, the results tend to settle down nicely as the

maximum available number of sweeps is reached. Based on the preceding results and discussion, the chosen number of 160 sweeps seemed to be reasonable within the storage area available during the test.[11]

The chordwise variation of the mean axial velocity at seven different radial stations is shown in Fig. 12. The horizontal axis of Figs. 12-19 represents the blade chord at each blade radius. The leading- and trailing-edge positions are marked on each of the figures. The propeller imparts energy to the flow downstream, which implies that the axial velocity ratio U/U_∞ is greater than 1.0 on the average over the disk. The probe senses lower air velocities whenever a blade passes the probe. This is the reason for having local wake defects in the profiles shown here. At the tip, a relatively big defect was observed. The velocities are very nearly constant outside the blade wakes.

It was found that the transverse velocity has a higher value directly behind the blade rather than outside it. Furthermore, the profile varies in magnitude along the blade chord, which could be used as an indication of the associated vortex sheet distribution. It was found that the signal representing the vertical component of mean velocity changes direction across the blade chord. To better illustrate this, a vector diagram was prepared in Fig. 13 to give an idea about flow directionality immediately behind the blade. From this graph, we see that the flow is mostly contracted for inner radii, and the opposite is true for outer radii (0.80-1.0R).

A high axial turbulence intensity $\sqrt{u'^2}/U$ region was found to exist near the hub, as well as at the tip sections, where turbulence levels reach as high as 40%, as shown in Fig. 14. At the tip, the turbulence level is relatively high and occupies a region extending outside the tip chord length in the trailing-edge direction. This is clearly due to the strong vortex shedding at the tip. The axial turbulence intensity level averaged circumferentially at a particular blade radius (0.8R) is only 5%, whereas in the region behind the blade at the same radius it ranges from 15 to 20%.

Figure 15 shows the turbulence intensity in the Y direction, $\sqrt{v'^2}/U$. Inner radii (0.36-0.55R) have a high turbulence level at about 14% starting from midchord. Another region of high turbulence level is at the tip region extending after the trailing edge.

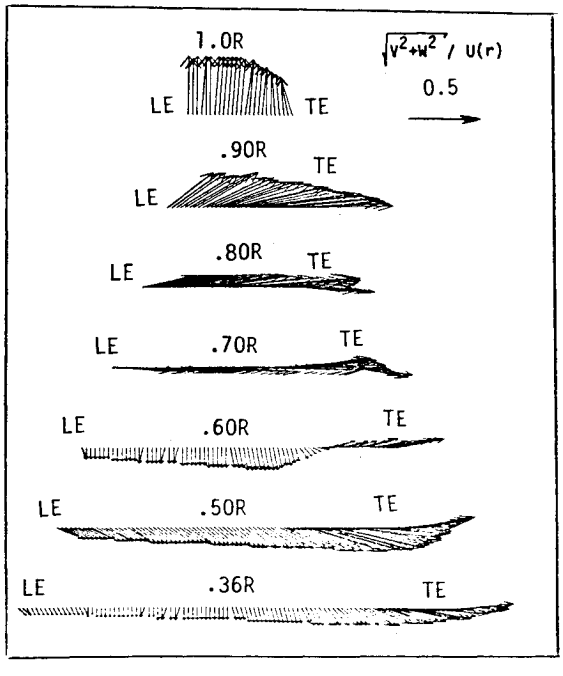

Fig. 13 Velocity field behind a propeller blade (YZ plane) in uniform flow at $J=0.899$.

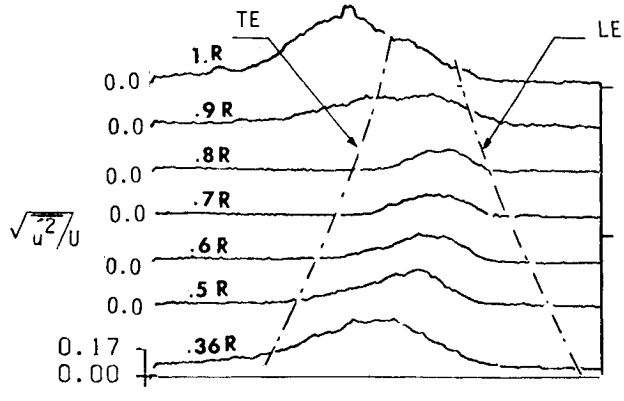

Fig. 14 Axial turbulence intensity profiles behind a propeller blade in uniform flow at $J=0.899$.

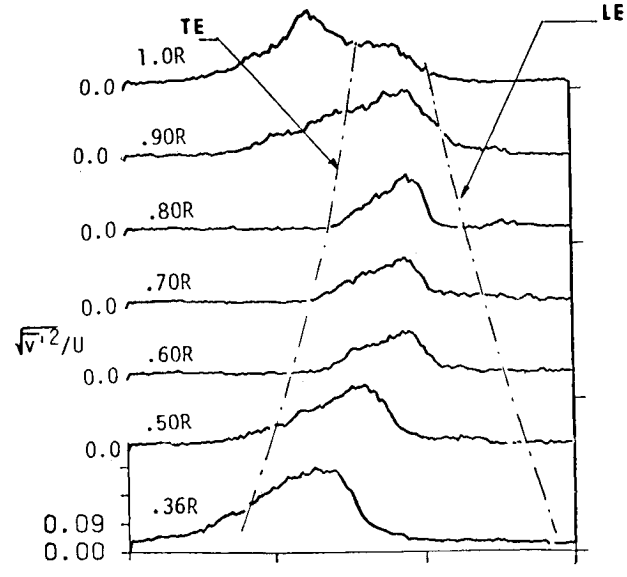

Fig. 15 Turbulence intensity profiles (Y component) behind a propeller blade in uniform flow at $J=0.899$.

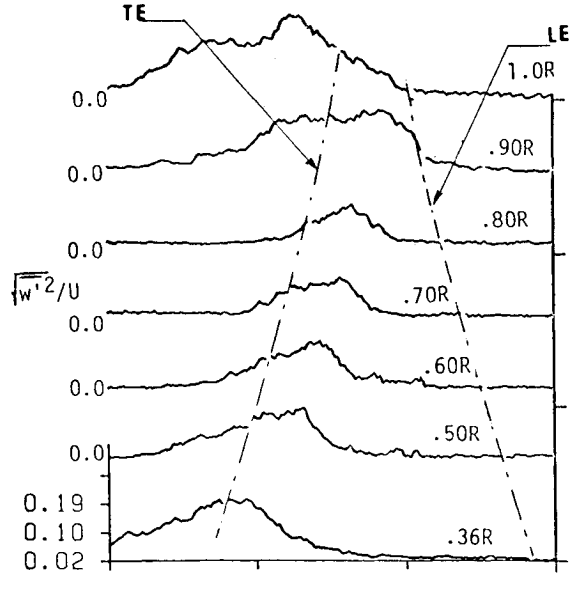

Fig. 16 Turbulence intensity profiles (Z component) behind a propeller blade in uniform flow at $J=0.899$.

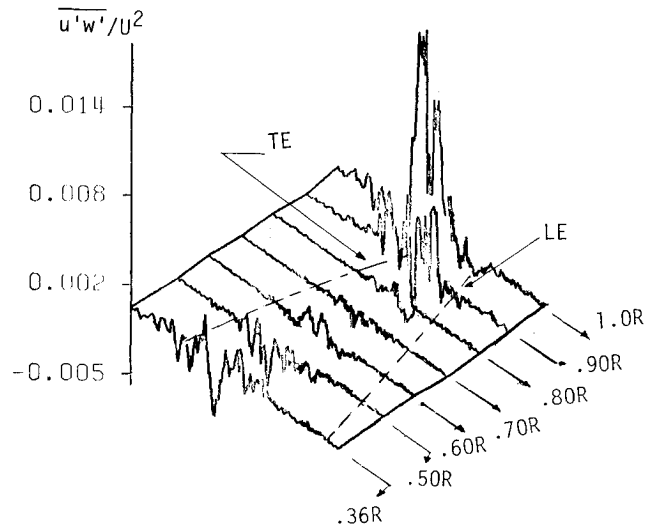

Fig. 17 Reynolds stress profiles ($\overline{u'w'}$ component) behind a propeller blade in uniform flow at $X/D=0.025$ and $J=0.899$.

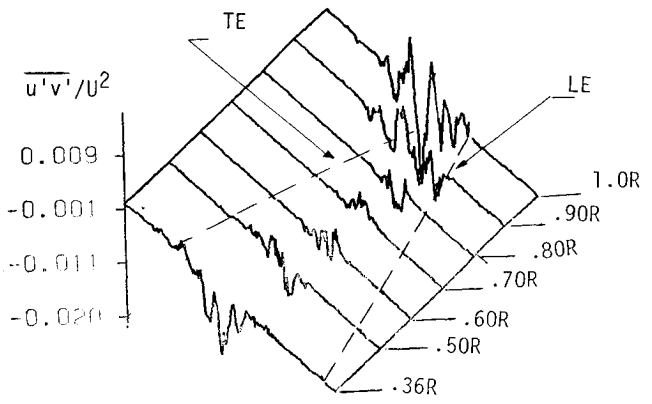

Fig. 18 Reynolds stress profiles ($\overline{u'v'}$ component) behind a propeller blade in uniform flow at $X/D=0.025$ and $J=0.899$.

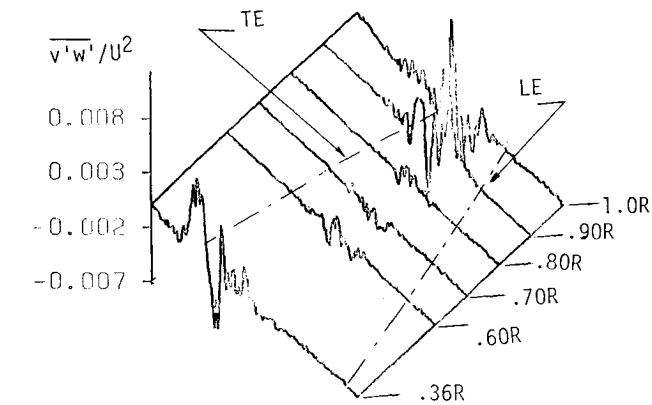

Fig. 19 Reynolds stress profiles ($\overline{v'w'}$ component) behind a propeller blade in uniform flow at $X/D=0.025$ and $J=0.899$.

The turbulence intensity in the Z direction, $\sqrt{w'^2}/U$, is given in Fig. 16. Except for a small portion of the blade region at $0.36R$ and the blade tip (0.85-$1.0R$), the turbulence level in the Z direction is relatively lower—less than 12%. The blade radius at $0.7R$ was selected to examine the ordering of the velocity fluctuations in the three directions measured. This section will be away from the tip or hub effects. It was found that the three turbulent components have almost the same level (maximum values are 12, 14, and 13.6% in the X, Y, and Z directions, respectively).

The hot-wire data have been reduced to yield the three Reynolds stress components, $\rho\overline{u'v'}$, $\rho\overline{u'w'}$, and $\rho\overline{u'v'}$, respectively, and are plotted in a normalized form using $\rho_\infty U^2$. Figure 17 gives the $\rho\overline{u'w'}$ component profiles. Excluding the tip region, all fluctuations and higher values are confined within the blade chord region. Spanwise, the middle radial stations (0.5-$0.8R$) assume the lowest levels.

The other two Reynolds stress components, $\rho\overline{u'v'}$ and $\rho\overline{v'w'}$, are given in Figs. 18 and 19. They exhibit the same general features.

Conclusions

Different experimental techniques were used to investigate propeller performance and influence on the surrounding flowfield. Starting with direct measurements of global parameters and ending with the spatial variation of mean and fluctuating flow quantities behind individual blades, a complete picture for the physical problem of propeller action was obtained. An intermediate step also was made; i.e., to measure flow quantities averaged in the circumferential direction. The results obtained through that step resembled an actuator disk simulation (infinite number of blades). This yielded what we call global "turbulence" measurements, including the effects of shed vortex sheets, etc.

The individual blade wake measurements clearly pointed out that although the flow behind the disk is axially accelerated overall, there are strong defects in the profiles directly behind the blades. Secondary flow (swirl and contraction) in the blade wake indicates a flow pattern associated with the bound and trailing vortex system.

The unsteadiness of the vortex sheet emanating from the blade was demonstrated clearly. Profiles representing the azimuthal variation of fluctuating quantities were periodic in nature. However, higher intensities were found within the blade wakes, while much lower values were observed outside the blade wake regions. Also, within the blade wake, the three components of the turbulent shear stresses increase toward the hub.

Finally, although the shear introduced to the freestream flow was not strong and the propeller did not respond significantly to the shear incident flow as far as global performance quantities are concerned, the different effects on the resulting detailed flowfields were documented.

Acknowledgments

This work was supported in part by the Office of Naval Research with Dr. Choung Lee as Technical Monitor.

References

[1]Schetz, J.A. and Stottmeister, H.R., "Experimental Measurements in the Near-Wake Region of a Self-Propelled, Slender Body with Attached Appendages, VPI & SU, Blacksburg, VA, VPI-Aero-077, Feb. 1979.

[2]Swanson, R.C., Schetz, J.A., and Jakubowski, A.K., "Turbulent Wake Behind Slender Bodies Including Self-Propelled Configurations," VPI & SU, Blacksburg, VA, VPI-Aero-024, 1974.

[3]Chieng, C.C., Jakubowski, A.K., and Schetz, J.A., "Investigation of Turbulent Properties of the Wake Behind Self-Propelled Axisymmetric Bodies," VPI & SU, Blacksburg, VA, VPI-Aero-025, 1974.

[4]Schetz, J.A., Daffan, E.B., Jakubowski, A.K., Cannon, S., Cox, R., and Dubberley, D., "Mean Flow and Turbulence Measurements in the Wake of Slender Propeller-Driven Bodies Including Effects of Pitch Angle," VPI & SU, Blacksburg, VA, VPI-Aero-050, 1976.

[5]Schetz, J.A., Daffan, E.B., Jakubowski, A.K., Cannon, S., Cox, R., and Dubberley, D., "Mean Flow and Turbulence Measurements in the Wake of Slender Propeller-Driven Bodies Including Effects of Pitch Angle," VPI-Aero-050, 1976.

[6]Kotb, M.A. and Schetz, J.A., "Detailed Turbulent Flowfield Measurements Immediately Behind a Propeller," Society of Naval Architects and Marine Engineers, Propellers' 84 Symposium, Virginia Beach, VA, May 1984.

[7]Lee, H. "Computational and Experimental Study of Trailing Vortices," Ph.D. Dissertation, VPI & SU, Blacksburg, VA, 1983.

[8]Champagne, F.H. and Sleicher, C.A., "Turbulent Measurements with Inclined Hot-Wires. Part II—Hot Wire Response Equations," *Journal of Fluid Mechanics*, Vol. 28, Pt. I, 1967, pp. 177-182.

[9]Bendat, J.S. and Piersol, A.G., *Random Data Analysis and Measurement Procedures*, Wiley-Interscience, New York, 1971.

[10]Bendat, J.S. and Piersol, A.G., *Measurement and Analysis of Random Data*, John Wiley & Sons, New York, 1966.

[11]Kotb, M.A., "Experimental Investigation of 3-D Turbulent Free Shear Flow Past Propellers and Windmills," Ph.D. Thesis, Aerospace and Ocean Engineering Department, VPI & SU, Blacksburg, VA, Nov. 1984.